Printing electrodes for P(VDF-TrFE-CTFE) actuators using a consumer grade inkjet printer

Baelz, K. Keith; Hunt, Andres

DOI
10.1117/12.2660469

Publication date
2023

Document Version
Final published version

Published in
Electroactive Polymer Actuators and Devices (EAPAD) XXV

PROCEEDINGS OF SPIE

SPIEDigitalLibrary.org/conference-proceedings-of-spie

Printing electrodes for P(VDF-TrFE-CTFE) actuators using a consumer-grade inkjet printer

K. Keith Baelz, Andres Hunt

K. Keith Baelz, Andres Hunt, "Printing electrodes for P(VDF-TrFE-CTFE) actuators using a consumer-grade inkjet printer," Proc. SPIE 12482, Electroactive Polymer Actuators and Devices (EAPAD) XXV, 124820P (28 April 2023); doi: 10.1117/12.2660469

SPIE.

Event: SPIE Smart Structures + Nondestructive Evaluation, 2023, Long Beach, California, United States

Printing electrodes for P(VDF-TrFE-CTFE) actuators using a consumer grade inkjet printer

K. Keith Baelz and Andres Hunt

Department of Precision and Microsystems Engineering, Delft University of Technology, Mekelweg 2, 2628CD Delft, The Netherlands

ABSTRACT

To facilitate smart material transducer research and application, it is important to develop fabrication processes that are widely accessible and compatible with additive manufacturing (AM) techniques. This work addresses inkjet printing and material selection in the fabrication of bending cantilever actuators based on the P(VDF-TrFE-CTFE) relaxor ferroelectric polymer. It investigates the effects of three different substrates (PEN, polyimide and a PET-based) and four different conductive inks (metal- and carbon-based) on the actuator fabrication and performance, to minimize process complexity and need for specialized equipment. First, electrode samples are manufactured for the feasible substrate-ink combination, their sheet resistances are measured, and their feasibility for actuator electrodes is analysed. Then, the simplest viable process is employed to fabricate the actuator samples, and their performance is measured in quasi-static and dynamic experiments. The least complex fabrication process was achieved with the resin-coated PET substrate (IJ-220) and carbon black electrodes (JR-700LV), only requiring a consumer-grade inkjet printer, a spin-coater and a thermal oven. The electrode samples showed $2.29 \cdot 10^3$ $\Omega/\square$ sheet resistance at 10 print repetitions, indicating an actuator's electrical bandwidth of 9.36 kHz. The manufactured actuators achieved 206 μm tip deflections in response to 1 Hz 300 V excitation, and up to 3 mm deflections in resonant operation at 115 Hz. Therefore, manufacturing flexible designs of well-performing smart material actuators is viable using widely available and low-budget equipment.

Keywords: Electroactive polymer, actuator, inkjet printing, electrodes, relaxor ferroelectric, P(VDF-TrFE-CTFE), carbon black, silver

1. INTRODUCTION

Inkjet printing is increasingly employed for printing of electronic circuits and components,[1,2] and it has enabled deposition of electrodes and electroactive polymer (EAP) layers in the fabrication processes of smart material sensors and actuators, e.g. printing carbon black electrodes for DEAs (dielectric elastomer actuators)[3] and P(VDF-TrFE) polymer for piezopolymer transducers.[4,5] This allows to speed up transducer manufacture, improve repeatability and facilitate fabrication of complex transducer geometries.[6,7] Reducing the need for specialized (and costly) equipment and skills are prerequisites for adaptation of smart material transducers in broader research and development activities.

Devising simple and accessible processes for fabricating smart material actuators and sensors that perform well is limited by the available materials and processes. While inkjet-printing can significantly facilitate the material deposition, complexity of the fabrication process further depends on the required pre-treatment and curing steps. These vary significantly among the available materials and the respective material-substrate interfaces. Fabricating a simple bending unimorph transducer topology (Figure 1) raises these challenges three times, i.e. in the fabrication of each of the 3 material layers, each on a different surface material. For electrode fabrication, the choice of available inkjet-compatible conductive inks is increasingly broad, ranging from metal nanoparticle dispersions to carbon-based inks and conductive polymers, that significantly vary in their conductivities and curing processes. The options for well-performing EAPs are much narrower. Among electronic EAPs, PVDF

Further author information: (Send correspondence to A.H.)
K.K.B.: E-mail: K.K.Balz@student.tudelft.nl
A.H.: E-mail: A.Hunt@tudelft.nl

Electroactive Polymer Actuators and Devices (EAPAD) XXV, edited by Herbert R. Shea, Iain A. Anderson, John D. W. Madden, Proc. of SPIE Vol. 12482, 124820P
 · 0277-786X · doi: 10.1117/12.2660469

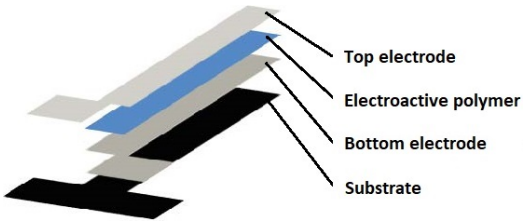

Figure 1. Topology of the bending smart material actuator.

copolymers (e.g. P(VDF-TrFE)) exhibit strong sensing phenomena, and the relaxor ferroelectric terpolymers of PVDF (e.g. P(VDF-TrFE-CTFE)) exhibit strong electrostriction, useful for actuation. Formulating these EAPs into printable inks poses first a challenges in chemical compatibility between the required harsh solvents and the printhead materials. Printing such inks poses another challenge in deposition speed, since the consumer grade printheads can rarely handle polymer concentrations above 1%[4,8] due to the high viscosity and non-Newtonian properties. This slows down the EAP deposition rate and makes the printing less attractive than the conventional techniques.

This research studies different combinations of substrates and conductive inks for manufacturing P(VDF-TrFE-CTFE) relaxor ferroelectric actuators on a consumer grade inkjet printer, aiming to reduce the complexity of the actuator fabrication and the need for specialized equipment. Using an Epson XP-900 printer as a manufacturing platform (Section 2.1), combinations of three common substrate materials and four inks of different types are studied (Section 2.2). Electrode samples are produced for all feasible combination and their sheet resistances are measured (Section 2.3). Their suitability for actuator electrodes is then evaluated by modelling the electrical behaviour of the actuator design (Section 2.4). For manufacturing the actuators we choose the electrode and substrate materials that are the least complex to manufacture among all the electrically feasible combinations. The actuators are then manufactured by inkjet printing the electrodes, spin-coating the EAP, and thermally curing both of them (Section 2.5). Actuation performance is measured in quasi-static and dynamic experiments (Section 2.6). Sections 3 and 4 respectively discuss the results and conclude this paper.

2. MATERIALS AND METHODS

This paper considers the unimorph design of a bending cantilever actuator, as explained in Figure 1. To assure high actuation performance, the actuators are based on the P(VDF-TrFE-CTFE) relaxor ferroelectric polymer, able to produce strains $> 5\%$.[9] To attain a robust and accessible actuator fabrication process this work uses a consumer grade inkjet printer for electrode deposition and a spin-coater for EAP deposition. The printing process and the required printer preparation are explained in Section 2.1. To choose the best suited substrate and electrode materials we explored the combinations of three substrate materials and four conductive inks, as specified in Section 2.2. The respective electrode sample fabrication and surface resistance measurements are described in Section 2.3. To evaluate sufficiency of these electrode conductivities for actuator electrodes we modelled their electrical behaviour, as explained in Section 2.4. Basing on the modelling results and fabrication complexity, the substrate and electrode materials are chosen. Actuator samples were then manufactured and characterized according to Sections 2.5 and 2.6, respectively.

2.1 Printer preparation and printing process

Conductive electrodes for the actuators were printed in this study using an Epson Expression Premium XP 900 printer (see Figure 2.a). The choice for this printer based on three key properties: (1) piezo-actuated printing chambers (as opposed to thermal inkjet)[10] that allow using inks that do not contain volatile solvents; (2) the feature of printing on CDs, whereas the CD printing tray serves as the flat substrate table, where the target samples can be attached, eliminating the need for physically altering the printer; and (3) availability of refillable cartridges with auto-resetting ink counter, that allowed using custom inks without the need for pre-cleaning and occasional chip resetting (ink counter). Suitability of the commercial printers for depositing custom inks further depend on the rheological properties[11] and solvent composition of the inks. Correspondingly, they determine if the ink is jettable and chemically compatible with parts of the printer that it comes in contact with.

Printer preparation starts with removing the internal pads from the refillable cartridges to facilitate their cleaning. Next, larger openings are cut on the top of the cartridges to facilitate the loading and unloading of the inks. These alterations are made for the ease of servicing, and are not essential. Since the printer uses 3 color (plus 2 black) cartridges, then multiple conductive inks can be loaded simultaneously. Printing process starts with inserting the refillable cartridges and loading them with conductive inks via a PTFE syringe filter (5 μm for JR-700LV, 0.45 μm for the other inks). If needed, the cartridges can be emptied and the printhead can be cleaned by loading it with a purging solution (mixture of DI water, glycerol and ethylene glycol) and setting the printer into a cleaning cycle. We observed better results and less need for service procedures when allowing the newly loaded ink to settle overnight within the printhead before printing.

We permanently fixed a CD in the CD printing tray and used it as the printbed for attaching the substrate samples (blue masking tape, 3M), as shown in Figure 2.b. Alignment markers are printed on the CD to properly align the substrate on the printbed. The necessary print pattern is prepared as a PNG image in the color that corresponds to the cartridge of the conductive ink (magenta, cyan, yellow or black), and printed using the Epson Print CD software. Printing multiple repetition must be implemented manually, i.e. by re-inserting the tray with the same sample.

2.2 Actuator materials

Substrate properties influence its interactions with the deposited material (e.g. wettability and adhesion strength), and compatibility with the preparation and curing processes. In this study we chose three common substrates for printed actuators: 50 μm thick PEN film (polyethylene naphthalate, from Goodfellow),[12] 50 μm thick Kapton film[13] (polyimide) and 140 μm thick PET (polyethylene terephthalate) film with microporous resin coating (Novele IJ-220, Novacentrix).[14] The latter is specifically designed for printing conductive nanoparticle inks.

Four conductive inks were chosen basing on their suitability for printing on consumer grade inkjet printers: (1) 25% Ag nanoparticle dispersion ink JS-B25P from Novacentrix;[15] (2) 3.5% carbon black nanoparticle dispersion ink JR-700LV from Novacentrix;[16] (3) 10% copper oxide nanoparticle dispersion ink ICI-003 from Novacentrix;[17] and (4) 15% Ag nanoparticle dispersion ink NBSIJ-MU01 from Mitsubishi Paper Mills Ltd.[18] Novacentrix indicates that JS-B25P can be sintered thermally or photonically, ICI-003 only photonically, JR-700LV doesn't require sintering if printed on the Novele IJ-220 substrate, and the same is true for NBSIJ-MU01 ink.*

This study based on the Piezotech RT-TS poly(vinylidene fluoride-trifluoroethylene-chlorotrifluoroethylene) electroactive polymer (P(VDF-TrFE-CTFE) in short, from Arkema).[9] It serves as the source of electromechanical transduction within the actuator structure and can exhibit strains above 5%.[9] To prepare the polymer solution for spin-coating, the polymer powder was dissolved in butanone (SigmaAldrich) in the ratio of EAP 1:10 butanone, and air bubbles were removed from the solution using a desiccator. Desiccator is not needed if the polymer is not mixed, but dissolving takes then several hours.

*The IJ-220 substrate is manufactured for NovaCentrix by Mitsubishi Imaging (MPM), Inc, a division of the producer of the NBSIJ-MU01 ink.

a. b. c.

Figure 2. Inkjet printing of the conductive inks: a. The Epson XP 900 printer, b. the printbed with the printed samples mounted on it, and c. atest samples for studying conductivity of different ink and substrate combinations.

2.3 Electrode resistance

Electrical resistance of the electrodes affects the actuator performance via limiting the current and thus formation of the electric field across the electroactive polymer layer. To evaluate the significance of the electrode resistance on the actuator performance we investigated how the substrate-electrode material combinations and the number of printed electrode layers affect the electrode sheet resistance. In this study we: (1) manufactured 10-layer test samples of each of the feasible substrate-electrode combinations and measured their sheet resistances, and (2) chose the most promising substrate and fabricated test samples with different number of printed layers (i.e. 1 to 10) of all feasible inks on this substrate. The sample fabrication process is described in Section 2.3.1 and measuring the sheet resistances is explained in Section 2.3.2.

2.3.1 Fabrication

Fabrication stage of each of the test samples consisted of printing an electrode material onto a substrate sample, and if needed then also its curing. We based on the inks and substrates described in Section 2.2 and printed test samples of each of their feasible combination using methodology described in Section 2.1. The test samples were rectangles of conductive material with the dimensions of 15 mm by 20 mm, printed on a slightly larger substrate (see Figure 2.c).

Post-processing on the Kapton and PEN samples followed an identical procedure. For the carbon black ink the samples were placed in an oven (Memmert UN30) and kept at $80°C$ until evenly matte (ca 2h). Thermal curing of the other inks would require temperatures that damage the polymer substrates, and they were therefore photonically sintered. For this purpose we used a 355 nm pulsed laser (Spectra-Physics Talon 355-15) of a laser micromachining system (Optec WS Starter). The laser is set 10 mm out of focus (resulting the spot diameter of 1.28 mm) to prevent damage from the excessive fluence. The laser spot followed the hatch pattern with 6 μm line spacing on the electrode layout (50 kHz pulse repetition rate, 3 A current, 150 mm/s speed, 4 passes).

2.3.2 Sheet resistance

To compare the conductivity between the different ink and substrate combinations, the sheet resistances of the electrodes samples was measured using a 4 point probe with the Signatone SP4 probe head (1.58 mm electrode spacing). 10 μA was supplied to the outer electrodes using a current source (Keithley 2400 SourceMeter), and the voltage was measured between the inner electrodes (Keithley 2182 Nanovoltmeter).

Since the probe electrode spacing is much larger than the film thickness t ($\approx 1\ \mu m$) and much smaller than the sample dimensions, then using geometric correction factor $R_1 = 0.9223$,[19] the sample sheet resistance can be calculated as:

$$R_s = \frac{\rho}{t} = \frac{V \pi R_1}{I\ ln(2)} \approx 4.18 \frac{V}{I}, \tag{1}$$

where ρ is the electrode resistivity, I is the applied current and V is the voltage reading.

2.4 Modelling the electrical behaviour

Viability of the printed conductor layers for actuator electrodes was evaluated by modelling the electrical behaviour of the actuator. We used a lumped RCR ladder equivalent circuit model, where the electrodes and the EAP layer are represented as resistances and capacitances. The model considers only this portion of the design as an actuator where all three layers (i.e. the EAP and both electrodes) have been deposited on the substrate (Figure 1. A 5-element model was constructed in Simscape environment (Matlab), as shown in Figure 3. The electrodes serve both as the capacitor electrodes and resistors in the actuator length direction, and the EAP layer as the dielectric between the capacitor electrodes. For each segment of the actuator with a cross-sectional area A and length L, we can obtain the resistances (for the top and bottom electrodes) and the capacitance:

$$R = \frac{R_s t L}{A}, \quad C = \frac{\epsilon L W}{d}, \tag{2}$$

where W is the width of the actuator, ϵ is the dielectric permittivity of the EAP, and d is the EAP layer thickness. Resistance parameters were obtained from the sheet resistance measurements, while the capacitances were too small to reliably measure, and were therefore calculated from the EAP dimensions and properties.

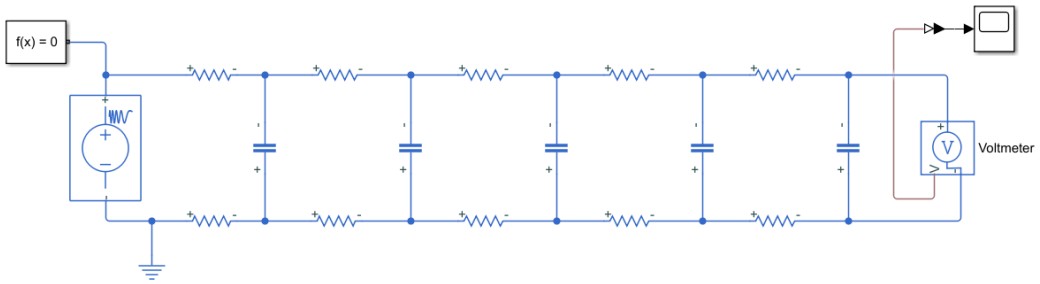

Figure 3. Modelling the electrical behaviour of the bending actuator using a lumped RCR ladder equivalent circuit model. The 5-element model is implemented in Simscape environment (Matlab Simulink) to estimate the voltage at the tip of the actuator (on the right) in response to the step excitation at its base (left).

The simulations allow to extract the time constant τ for the voltage rise on last segment of the ladder model (i.e. actuator tip) in response to applying a step input voltage on the first segment (i.e. actuator base). Then the bandwidth ($-3\ dB$) frequency for the signal on the actuator end segment is given by:

$$f_{3dB} = \frac{1}{2\pi\tau}. \tag{3}$$

If this bandwidth is much higher than the first mechanical resonance of the cantilever actuator, then the contribution of the surface resistance effects on the actuator performance can be considered negligible.

2.5 Actuator manufacture

For experimental validation of the electrode study outcomes we manufactured EAP actuators according to the design and morphology described in Figure 1. The long cantilever beam functions as a bending unimorph actuator, and its base (inverted-T shape) allows the mechanical clamping and making the electrical connections. The actuator manufacture was based on the carbon black ink and the PET substrate (IJ-220), that proved the most suitable in the experiments and modelling, as later explained in Sections 3.3 and 3.4. Fabrication of the actuators consisted of the steps for depositing and curing of the bottom electrode, the EAP layer and the top electrode, as follows:

(1) Bottom electrode: Six layers of the carbon black ink (JR-700LV) were printed on the resin-coated PET substrate (IJ-220) as described in Section 2.1. This resulted in an even coverage, where the substrate turned from translucent to opaque. The sample was then heated in an oven (Memmert UN30) at 80 deg for 30 min to evaporate the ink solvent residues.

(2) Electroactive polymer layer: Three layers of the EAP solution were spin-coated on the bottom electrode, and then thermally annealed. The EAP solution (preparation in Section 2.2) was applied by a pipette to cover the entire bottom electrode, and allowed to wet the electrode for 30 s. The sample was then spinned for 30 s at 1500 rpm (Polos SPIN150i), followed by a 5 min settling time to allow the solvent to evaporate, before applying the next layer. After applying 3 layers, the sample was annealed in an oven (Memmert UN30) for $2h$ at $111°C$. For the EAP layer fabrication, spin-coating is used instead of inkjet printing, since jettable EAP inks should be $< 1\%$ in polymer concentration, that would require hundreds of print repetitions to deposit a sufficient layer thickness.

(3) Top electrode: Ten layers of the carbon black ink were printed directly on the EAP layer (no surface pre-treatment), as explained in Section 2.1. Unlike on the porous substrate, the EAP did not absorb the solvents, and the ink did not wet the surface, requiring more repetitions to attain an even coverage. After printing, the solvent was evaporated by heating the sample to $80°C$ for 30 min, turning it matte black in appearance.

After manufacture, the actuators were also poled to produce piezoelectric behaviour and to increase their electromechanical transduction. Actuators were placed on a hotplate (Stuart UC150) and heated to $85°C$. Once the temperature was reached, 140 V was applied on their electrodes (Delta Elektronika ES300) for 20 min, and then the hotplate was turned off. Once cooled down to the room temperature, the voltage was turned off and the samples are removed. Excessive substrate material was removed by a scalpel to finalize the actuators.

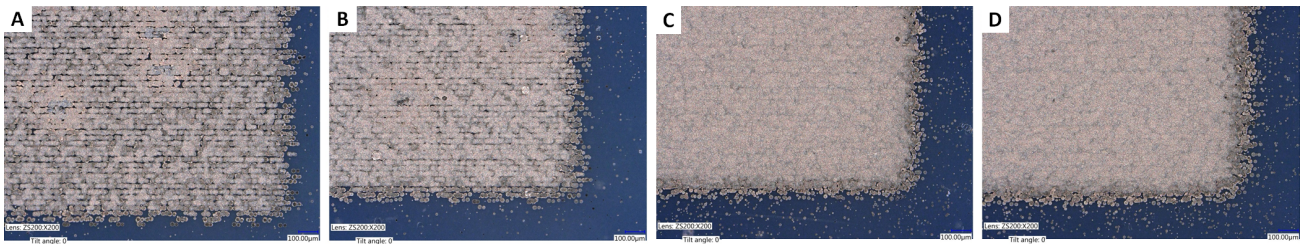

Figure 4. The effect of the printing repetitions on the quality of the electrodes. Sintered electrode samples of the JS-B25P ink on the Novele IJ-220 substrate after depositing (A) 2 layers, (B) 3 layers, (C) 4 layers, and (D) 5 layers of the ink.

2.6 Actuator characterisation

For characterisation, we measured the actuator deflections upon quasi-static excitation (1 Hz sine wave), the (mechanical) first resonant frequency of the actuator, and the corresponding actuator displacement range. Actuator was powered via a high-voltage amplifier (Smart Materials HVA 1500/50) and its deflections were measured using a laser distance meter ($\mu\epsilon$ optoNCDT ILD1750-2). The excitation signal was produced by a signal generator (RS Pro RSDG830) and the voltage and displacement data were collected via a NI USB-6211 data acquisition board in a PC computer with NI LabView 2018 software.

3. RESULTS AND DISCUSSION

The results of this research are presented and discussed as follows. Section 3.1 addresses the manufacturing outcomes of the substrate-electrode combinations. Sheet resistance measurements of these electrode samples are addressed in Section 3.2. Section 3.3 covers the modelling results of the actuator's electrical behaviour. Finally, the results for manufacturing of the actuators and their experimental validation are reported and discussed in Section 3.4.

3.1 Electrode samples

Electrode samples were manufactured as explained in Section 2.3.1, and then inspected using an optical microscope (Keyence VHX-6000) and a white light interferometer (Bruker Contour GT-K 3D). The following subsections will describe the observations by each of the four inks.

3.1.1 Silver ink JS-B25P

Figure 4 shows the intermediate results for printing the JS-B25P ink on the Novele (IJ-220) substrate, indicating that it takes approximately 5 passes to homogeneously cover the substrate. Topography measurement on a smaller sample (2.5 mm wide electrode strip print) in Figure 5 shows that this achieves an approximately 0.6 μm thick coating. After the sintering, the sample turns from a dull grey to a slightly yellow tone, as shown in Figure 6. Best results for sintering the 5-layer electrode were attained using the laser settings given in Section 2.3.1. For the samples with more than 5 layers, the laser mean power was scaled up proportionally to the printed layer count.

Printing the JS-B25P ink on the non-porous Kapton and PEN substrates was more complicated due to the hydrophobic behaviour of these materials, requiring 8-10 print layers to achieve a sufficient coverage. This can be alleviated via functionalizing the surfaces by oxygen plasma treatment.[20] If unavailable, it is necessary to prevent the static electricity build-up and to maintain the substrate sample as uncontaminated as possible. For preparation, we treated the Kapton and PEN samples in a water 5:1 fabric softener solution, rinsed in 2-propanol, blew dry with compressed air and removed any final residues using a cotton ball stick. To prevent static electricity build-up within the printer we coated the printbed (i.e. the CD and the tray) with fabric softener and allowed it to dry.

After printing the ink remained visibly uneven and wet on the Kapton and PEN substrates. Upon sintering it turned from dark brown to grey in color, but showed significant variations in appearance (i.e. visibly brighter and darker areas) and conductivity due to the non-uniform layer thickness. On the Kapton substrate the printed material was successfully sintered despite the uneven coverage, as shown in Figure 7.a. However, sintering on the

PEN substrate remains a challenge due to its poor heat tolerance. Using settings where the laser power remains below the threshold of damaging the substrate does not successfully sinter the ink, and using sufficient power to sinter the ink causes the PEN surface to shrink and the conductive layer to crack (Figure 8).

3.1.2 Carbon black ink JR-700LV

Printing and curing the JR-700LV ink on the Novele IJ-220 substrate (see Section 2.3.1) resulted in a dark matte coating that could not be studied using a white light interferometer, and was difficult to evaluate under an optical microscope. An evenly opaque coating was achieved after printing 6 ink layers, as shown in Figure 7.b. Printing the carbon black ink on the Kapton and PEN substrates results in an even coating with small imperfections. The low-viscosity ink cannot wet the hydrophobic substrates, resulting in local pinhole defects. Before solvent evaporation we patched these defects by manually pulling the wet ink film together at the defect locations, using a small needle.

Printing of the JR-700LV ink was more challenging than the other inks due to the more frequent clogging and need for cleaning. While the small particle sizes (desirably $< 50\ nm$) make the metal inks stable, the carbon black ink with larger particles suffers from more pronounced sedimentation and aggregation effects.[21] We also observed that the printer seems to deposit significantly smaller ink droplets in the CD printing mode, than when printing on paper, and implements more frequent service procedures.

3.1.3 Copper oxide ink ICI-003

Two samples of the copper oxide ink were printed on the Novele IJ-220 substrate, respectively consisting of 5 and 10 layers of ink. Unfortunately it was not possible to establish a working laser sintering recipe for these samples, and they did not become conductive. Microscopy images of the two samples after the sintering attempts are shown in Figure 9. Due to the lack of suitable sintering equipment we did not proceed with this ink to the other substrates.

3.1.4 Silver ink NBSIJ-MU01

The Mitsubishi NBSIJ-MU01 ink was only printed on the Novele substrate. This ink is formulated to chemically self-sinter, and specifically requires the Novele IJ-220 substrate for this. Even coverage of the substrate was achieved after printing 5 layers, resulting immediately in a shiny silver appearance.

3.2 Electrode resistance

All the conductor-substrate test samples were measured for their sheet resistance using a 4 point probe method described in Section 2.3.2. Table 1 compares the average results over the 10 measurements for the test samples with 10 printed layers of ink on the substrate. This includes all feasible combinations of the three inks (JS-B25P, JR-700LV and NBSIJ-MU01) and the three substrates (PEN, Kapton, Novele). The copper oxide ink (ICI-003) was omitted since it could not be sintered with the available equipment. It requires a light source in

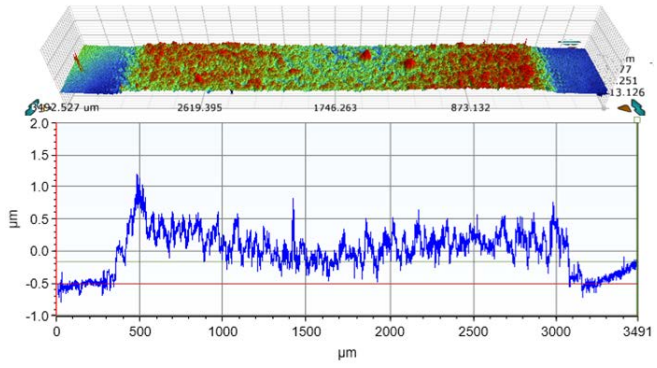

Figure 5. White light interferometer image of the electrode topography. 5 layers of silver ink (JS-B25P) were printed on the Novele substrate, prior to sintering.

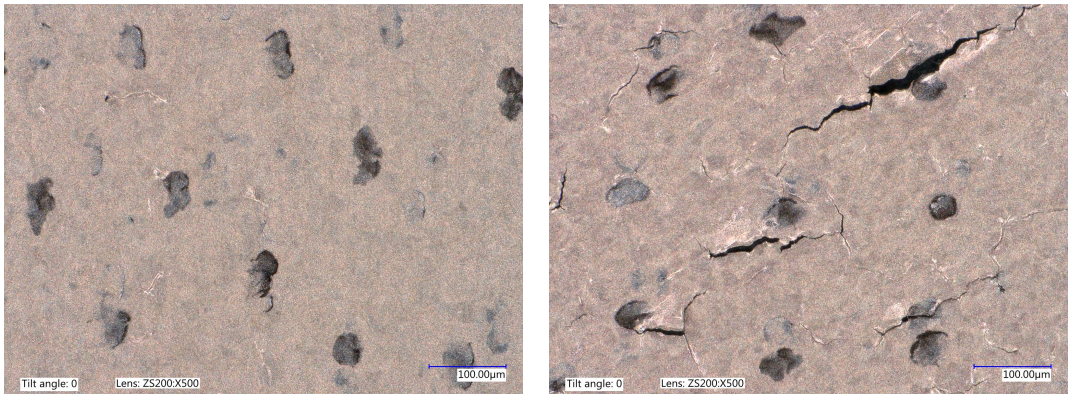

a. b.

Figure 6. Sintering the JS-B25P silver ink on the Novele substrate: a. five layers, after successful sintering, and b. four layers, after excessive sintering.

the $808 - 1064\ nm$ range that was not available in this study.[17] The NBSIJ-MU01 ink (Mitsubishi) requires a special substrate for chemical self-sintering, and was therefore only printed on the Novele IJ-220 substrate.

The effect of the printed layer count on the electrode sheet resistance was studied for the three feasible inks printed on the Novele substrate (IJ-220). While already a single layer of the silver inks (NBSIJ-MU01 and JS-B25P) produces measurably conductive electrodes, conductivity of the carbon black ink (JR-700LV) becomes measurable only after printing 2 layers. Therefore the sheet resistances were measured for the range of $2 - 10$ layers, and the results together with the standard deviations (over 10 measurements) are plotted in Figure 10. Here, the results showed exponentially decaying sheet resistances as more material is added. This is most probably caused by the incrementally increasing overlapping of the printed droplets, causing the electrode to start to behave as a bulk material as more material is added.

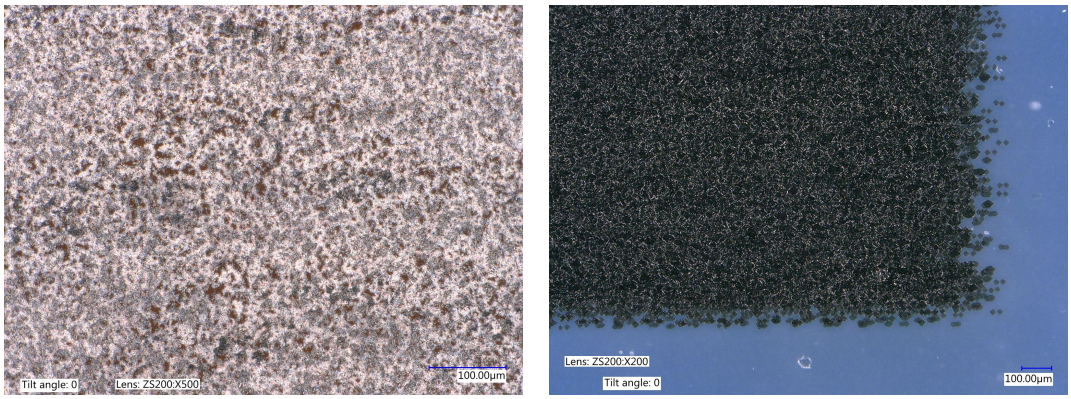

a. b.

Figure 7. Printing results: a. 10 layers of the JS-B25P ink on the Kapton substrate post-sintering, and b. 6 layers of the JR-700LV ink on the Novele substrate (untreated).

Table 1. The sheet resistance measurement results for each feasible ink and substrate combination after printing and post-processing 10 layers of ink. The averages and standard deviations over 10 measurements are given.

	Substrate		
Ink	**Novele**	**PEN**	**Kapton**
JS-B25P	$4.950(139) \cdot 10^{-2}\ \Omega/\square$	$2.56(307) \cdot 10^{3}\ \Omega/\square$	$1.060(253)\ \Omega/\square$
JR-700LV	$2.2880(281) \cdot 10^{3}\ \Omega/\square$	$2.0983(973) \cdot 10^{3}\ \Omega/\square$	$2.151(131) \cdot 10^{3}\ \Omega/\square$
NBSIJ-MU01	$1.0500(344) \cdot 10^{-1}\ \Omega/\square$	n/a	n/a

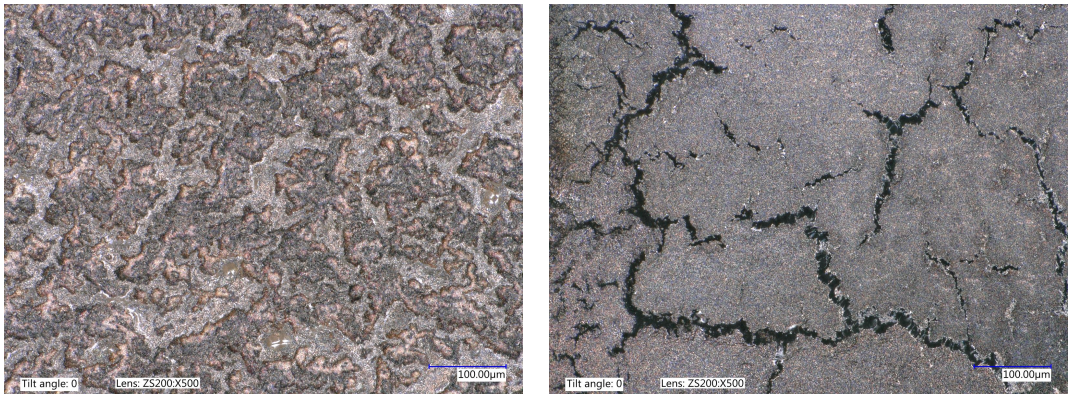

a. b.

Figure 8. Printing 10 layers of the conductive silver electrode (JS-B25P) on the PEN substrate: a. an under-sintered sample does not conduct electricity, and b. an over-sintered sample is damaged.

Printing 10 layers of the JS-B25P ink (on the IJ-220 substrate) resulted in a sheet resistance of 50 $m\Omega/\square$ after sintering, which is lower than the 100.3 $m\Omega/\square$ reported in the ink datasheet[15] (print settings and layer count not specified). Notably, the JS-B25P ink also became conductive immediately after printing, and did not improve significantly upon sintering, as shown in Table 2. The NBSIJ-MU01 ink (on the IJ-220 substrate) attained the sheet resistance of 0.105 $\Omega/\square$, that is somewhat better than the 0.19 $\Omega/\square$ reported for similar substrates in.[1]

Printing the JR-700LV ink (on the IJ-220 substrate) resulted in the sheet resistances below 2.5 $k\Omega/\square$ for 10 layers. Similar ink to JR-700LV has been reported to attain sheet resistance of 13 $k\Omega/\square$ for an approximately 1 μm thick electrodes (2 printed layers).[3] This is similar to the 2 and 3 layer values of the JR-700LV ink in Figure 10, but our electrode thickness could not be measured.

3.3 Modelling

Modelling the electrical behaviour of the actuator (Figure 3) based on the methodology described in Section 2.4, and the actuator topology shown in Figure 1. Dimensions of the actuator therefore are 2.7 mm by 17.5 mm. For the electrode resistances we used the values for the JR-700LV ink, since it was the least conductive, allowing to evaluate the electrical behaviour of the actuator in the worst case scenario. The bottom electrode resistances were derived from the sheet resistance measurement results for the 7-layer thick carbon black ink (JR-700LV) on the Novele substrate (IJ-220), i.e. 3165 $\Omega/\square$ (Figure 10). To derive the top electrode resistances, we assume the carbon black ink to behave on top of the EAP layer similarly to the Kapton and PEN substrates, since they

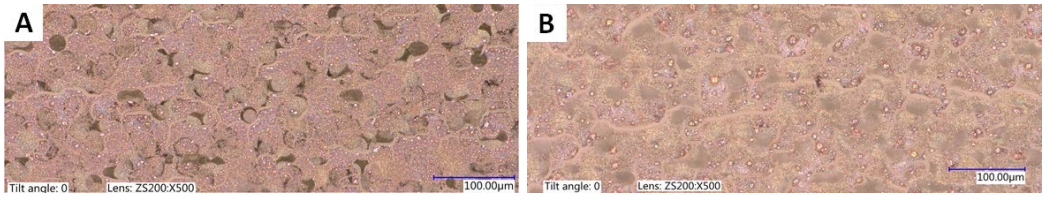

Figure 9. Sintering the copper ink (ICI-003) on the Novele substrate did not succeed: A. 5 layers, and B. 10 layers, post-sintering.

Table 2. Sheet resistances of the JS-B25P silver ink on the Novele IJ-220 substrate, pre- and post-sintering.

	Sheet resistance		
	4 layers	**5 layers**	**6 layers**
Unsintered sample	0.167 $\Omega/\square$	0.136 $\Omega/\square$	0.0923 $\Omega/\square$
Sintered sample	0.138 $\Omega/\square$	0.100 $\Omega/\square$	0.0857 $\Omega/\square$
Improvement	17.6%	26.3%	7.15%

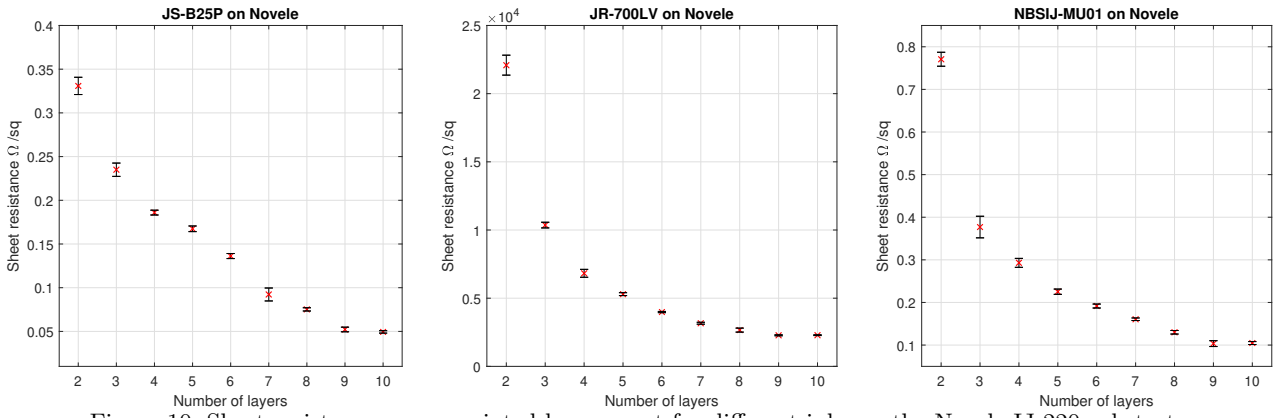

Figure 10. Sheet resistance versus printed layer count for different inks on the Novele IJ-220 substrate.

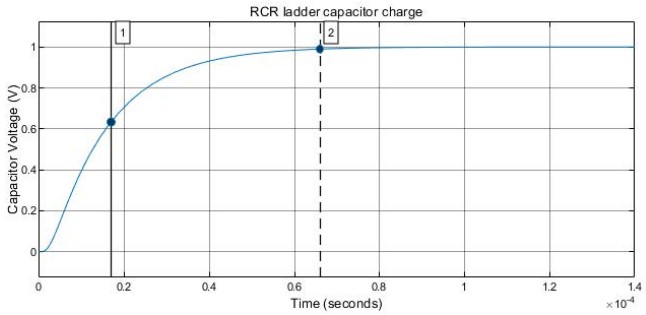

Figure 11. Simulation results for the voltage at the tip of the actuator (see model in Figure 3) upon a step excitation at its base.

all are non-porous. Since the ink showed lower conductivity on the PEN than on the Kapton substrate, then we derived the top electrode resistances from the PEN sheet resistance measurement results for 10 layers of the carbon black (Table 1). Layer count (7 and 10, respectively for the bottom and top electrodes) was chosen basing on the manufacturing observations (Section 3.1) and the resistance measurement results (Section 3.2), such that an even coverage would be achieved without significant manufacturing imperfections (e.g. pinhole defects). The actuator capacitance was calculated from its surface area, thickness (measured 22 μm) and relative permittivity ($\epsilon_r = 45$[9]).

The simulation applied a 1 V step input, and the resulting voltage response on the last capacitor of the RCR ladder circuit is plotted in Figure 11. The resulting charging time constant (i.e. the time to reach $1/e$ of the applied amplitude) was $1.70 \cdot 10^{-5}$ s, and the voltage reached 99% of the input voltage after $6.61 \cdot 10^{-5}$ s. This means that the -3 dB electrical bandwidth is 9362 Hz, which is almost two orders of magnitude higher than the first mechanical resonance of the actuator beam (i.e. ca 100 Hz). Therefore it is feasible to use any of the electrode manufacturing recipes from our selection that became conductive, without significantly impacting the actuator performance.

3.4 Actuators

The results of the actuator manufacture are addressed on Section 3.4.1, followed by the performance characterization in Section 3.4.2.

3.4.1 Manufacturing

The actuators were manufactured according to Section 2.5, and are shown in Figure 12. We implemented the simplest process that produces well-performing actuators, with the least need for specialized equipment. Therefore the chosen process based on the Novele IJ-220 substrate, inkjet printing of the carbon black electrodes (from the JR-700LV ink), and spin-coating of the P(VDF-TrFE-CTFE) electroactive polymer solvent. The rationale behind such choice is explained in the following.

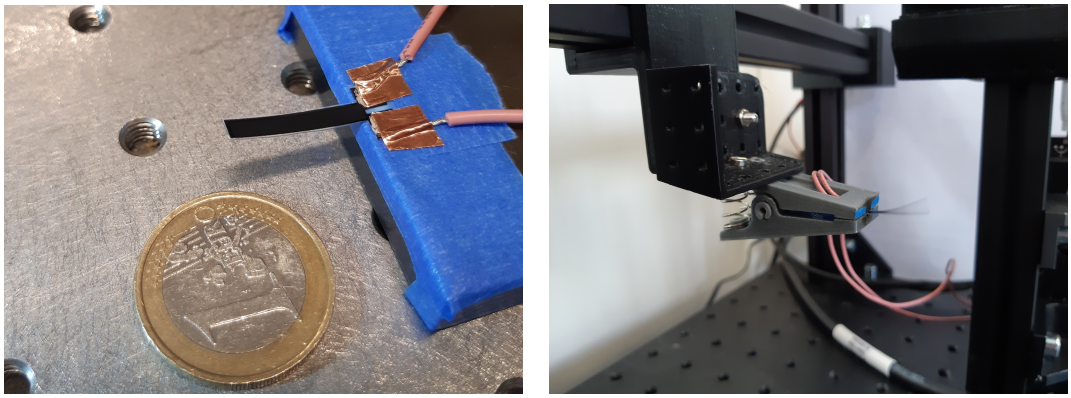

a. b.

Figure 12. Actuator samples: a. testing of their functionality, and b. Video 1 shows measuring their response to sinusoidal excitation http://dx.doi.org/10.1117/12.2660469.1.

The Novele IJ-220 substrate simplifies the fabrication process regardless of the ink, since only minor post-processing is required for the JR-700LV ink, and none for the NBSIJ-MU01 and JS-B25P inks. The ICI-003 ink could not be sintered using the available equipment;

The JR-700LV carbon black ink requires drying at $80°C$ for curing, which remains well below the substrate melting point ($122°C$). While the silver inks (NBSIJ-MU01 and JS-B25P) did not require any curing on the Novele IJ-220 substrate, they remained non-conductive and wet in appearance after printing on the EAP (i.e. when printing the top electrode), and required sintering. The latter is unfortunately either incompatible with the substrate (e.g. due to the high temperatures) or requires specialized equipment (e.g. for photonic sintering). Both the top and bottom electrodes can therefore be printed and cured using the JR-700LV ink. The modelling in Section 3.3 estimated the electrical bandwidth of 9362 Hz, indicating that the lower conductivity of the JR-700LV electrodes does not affect the actuator functionality. Other benefits of using the carbon black ink include its affordability and safety. It is the most affordable one from all the studied inks, and since the carbon black particles are not fused together, then their impact on the actuator stiffness is insignificant. Furthermore, the particle size distribution within the JR-700LV ink places it in the microparticle category in terms of safety, that otherwise is a significant concern for the (metal) nanoparticle dispersion inks. Due to the larger particle sizes, the JR-700LV ink caused occasional clogging of the printhead and required much more frequent printer maintenance than the other inks.

The EAP layer was deposited using the spin-coating process, as described in Section 2.5. Spin-coating was chosen over inkjet printing since it proved impossible to formulate printable polymer inks with the P(VDF-TrFE-CTFE) polymer concentrations above 1%, and all our attempts resulted in the ink polymerizing within the printhead, causing it to fail. Printing hundreds of layers of the low-concentration inks would also be unreasonably time-consuming, while spin-coating only takes about 20 min (excluding the curing time).

3.4.2 Characterization

After fabfication, the actuators were characterized as explained in Section 2.6. The maximum tip deflections for the unpoled and poled samples in response to 1 Hz sinusoidal excitation at 300 V amplitude were respectively measured to be 169 μm and 206 μm. As can be expected from the electrostrictive actuation of the polymer material, these experiments showed a quadratic response to the voltage stimulus and exhibited actuation hysteresis, as plotted in Figure 13. While the inverse piezoelectric effect (i.e. the result of poling) should not improve the actuation amplitude of the relaxor ferroelectrics in response to high excitation voltages, we hypothesize that the conditions of the poling process facilitated the formation of the β phase in the polymer, resulting in a stronger electrostrictive behaviour of the actuator samples after the poling. In the frequency response measurements the actuators achieved deflections of above 3 mm at the resonance frequency of 115 Hz. This is a significant improvement over the past results.[4,5] For a more elaborate description of the characterization process and the resulting performance measurements, the reader is refer to our report on actuator characterization.[22]

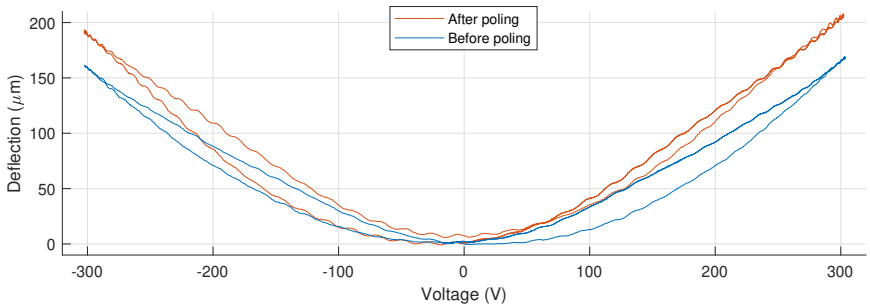

Figure 13. Actuation in responses to a bipolar sinusoidal excitation at 1 Hz and 300 V amplitude.

4. CONCLUSIONS

This paper proposed a methodology for simple and accessible fabrication of the bending actuators, basing on the P(VDF-TrFE-CTFE) EAP. We studied different combinations of substrates and inks to facilitate the deposition and curing processes of the actuator electrodes, using a consumer grade inkjet printer. Fabrication results indicated the Novele IJ-220 as the simplest substrate to work with for all inks, requiring no pre-processing. The carbon black ink JR-700LV turned out to be the easiest to deposit on the EAP, and only requires thermal curing at $80°C$, both on the EAP and on the IJ-220 substrate. Despite the highest sheet resistance ($2.29 \cdot 10^3\ \Omega/\square$ for 10 layers on IJ-220), the modelling of the electrical behaviour of the actuator indicated that the JR-700LV electrodes attain sufficient electrical bandwidth (9.36 kHz for $-3\ dB$), that is well above the first mechanical resonance of the actuator (115 Hz). The actuator samples were manufactured basing on the IJ-220 substrate by inkjet printing the carbon black (JR-700LV) electrodes, spin-coating the P(VDF-TrFE-CTFE) EAP, and thermally curing both the EAP and the electrodes ($111°C$ and $80°C$ respectively). The resulting actuators showed a very good performance for their type, achieving 206 μm deflections in response to quasi-static excitation (1 Hz sine, 300 V amplitude) and 3 mm deflections in resonant operation at 115 Hz, at 17.5 mm actuator length.

Therefore, manufacturing flexible designs of well-performing smart material actuators is viable using widely available and low-budget equipment. The process is low in complexity and bases on a consumer grade inkjet printer, a spin-coater and an oven. Carbon black ink is the most affordable of the investigated inks, and involves less safety concerns than the metal nanoparticle inks. Unfortunately spin-coating of the P(VDF-TrFE-CTFE) solution requires masking when fabricating more complicated designs, but is in general faster than inkjet-printing of the EAP. This study is expected to facilitate the broadening of the smart materials research and utilisation.

REFERENCES

[1] Kawahara, Y., Hodges, S., Cook, B. S., Zhang, C., and Abowd, G. D., "Instant inkjet circuits: lab-based inkjet printing to support rapid prototyping of ubicomp devices," in [*Proceedings of the 2013 ACM international joint conference on Pervasive and ubiquitous computing*], 363–372 (2013).

[2] Cui, Z., [*Printed electronics: materials, technologies and applications*], John Wiley & Sons (2016).

[3] Schlatter, S., Rosset, S., and Shea, H., "Inkjet printing of carbon black electrodes for dielectric elastomer actuators," in [*Electroactive Polymer Actuators and Devices (EAPAD) 2017*], **10163**, 1016311, International Society for Optics and Photonics (2017).

[4] Thuau, D., Kallitsis, K., Dos Santos, F. D., and Hadziioannou, G., "All inkjet-printed piezoelectric electronic devices: energy generators, sensors and actuators," *Journal of Materials Chemistry C* **5**(38), 9963–9966 (2017).

[5] Pabst, O., Perelaer, J., Beckert, E., Schubert, U. S., Eberhardt, R., and Tünnermann, A., "All inkjet-printed piezoelectric polymer actuators: Characterization and applications for micropumps in lab-on-a-chip systems," *Organic Electronics* **14**(12), 3423–3429 (2013).

[6] Andò, B., Baglio, S., Bulsara, A. R., Emery, T., Marletta, V., and Pistorio, A., "Low-cost inkjet printing technology for the rapid prototyping of transducers," *Sensors* **17**(4), 748 (2017).

[7] Perelaer, J. and Schubert, U., "8.07 - ink-jet printing of functional polymers for advanced applications," in [*Polymer Science: A Comprehensive Reference*], Matyjaszewski, K. and Möller, M., eds., 147–175, Elsevier, Amsterdam (2012).

[8] Haque, R. I., Vié, R., Germainy, M., Valbin, L., Benaben, P., and Boddaert, X., "Inkjet printing of high molecular weight pvdf-trfe for flexible electronics," *Flexible and Printed Electronics* **1**(1), 015001 (2015).

[9] Arkema, "Technical Guide Piezotech® RT-TS." Available online via: https://piezotech.arkema.com/en/Products/high-k-terpolymers. (Accessed: 1 March 2022).

[10] Bevione, M. and Chiolerio, A., "Benchmarking of inkjet printing methods for combined throughput and performance," *Advanced Engineering Materials* **22**(12), 2000679 (2020).

[11] Hutchings, I. M. and Martin, G. D., [*Inkjet technology for digital fabrication*], John Wiley & Sons (2012).

[12] Goodfellow GmbH, "Polyethylene naphthalate - Film." Online: https://www.goodfellow.com/de/en-gb/displayitemdetails/p/es36-fm-000150/polyethylene-naphthalate-film. (Accessed: 1 March 2022).

[13] DuPont, "DuPont™ Kapton® HN Polyimide Film." Online: https://www.dupont.com/content/dam/dupont/amer/us/en/products/ei-transformation/documents/DEC-Kapton-HN-datasheet.pdf. (Accessed: 1 March 2022).

[14] NovaCentrix, "Novele™ IJ-220 Printed Electronics Substrate - Inkjet Receptive." Online: https://www.novacentrix.com/datasheet/Novele%20IJ-220.pdf. (Accessed: 1 March 2022).

[15] NovaCentrix, "Metalon® JS-B25P Nanosilver Inkjet Ink – Aqueous dispersion for Dimatix and Epson Printheads." Online: https://www.novacentrix.com/datasheet/Metalon-JS-B25P-TDS.pdf. (Accessed: 1 March 2022).

[16] NovaCentrix, "Metalon® JR-700LV Carbon Ink – Aqueous dispersion for Inkjet Printing." Online: https://www.novacentrix.com/datasheet/Metalon-JR-700LV-TDS.pdf. (Accessed: 1 March 2022).

[17] NovaCentrix, "Metalon® ICI-002HV Nanocopper Ink - Aqueous dispersion." Online: https://www.novacentrix.com/datasheet/Metalon-ICI-002HV-TDS.pdf. (Accessed: 1 March 2022).

[18] Mitsubishi Paper Mills Ltd, "Silver Nano Particle Ink." Online: https://www.mpm.co.jp/electronic/eng/silver-nano/line-up.html. (Accessed: 1 March 2022).

[19] Topsoe, H., "Geometric factors in four point resistivity measurement," *Bulletin* **472**(13), 63 (1968).

[20] Sakai, Y., Futakuchi, T., and Adachi, M., "Preparation of batio3 thick films by inkjet printing on oxygen-plasma-modified substrates," *Japanese journal of applied physics* **45**(9S), 7247 (2006).

[21] Lau, G.-K. and Shrestha, M., "Ink-jet printing of micro-electro-mechanical systems (mems)," *Micromachines* **8**(6), 194 (2017).

[22] Baelz, K. K. and Hunt, A., "P (vdf-trfe-ctfe) actuators with inkjet printed electrodes," in [*2019 7th International Conference on Control, Mechatronics and Automation (ICCMA)*], 327–332, IEEE (2019).